Response to Anonymous Referee #2

We sincerely thank the Referee for the careful review and thoughtful comments, which are very helpful in improving our manuscript. We have addressed a point-to-point response to the comments and modified the manuscript accordingly. For clarity, the Referee's comments are reproduced in blue, authors' responses are in black and changes in the manuscript are in red.

The manuscript presents a compelling and timely investigation into the role of alkaline species, specifically ammonia and DMA, in modulating the chemical aging of SSA. By providing the first experimental evidence that these basic gases can significantly weaken chloride depletion, the study addresses a critical gap in our understanding of the coastal atmospheric chlorine cycle. The finding that acid-base neutralization serves as a primary regulatory mechanism for reactive chlorine species production is a significant contribution that could help reconcile discrepancies between observed and modeled chloride deficits in coastal regions.

1. Despite its innovation, the study's primary limitation lies in the concentration ranges employed; the use of 50–300 ppb of amines/ammonia significantly exceeds typical ambient levels (ppt to low ppb), which may exaggerate the observed inhibition effects and complicate the extrapolation to real-world conditions. Furthermore, while the study identifies organochlorines, the competitive kinetics between organic amine-acid neutralization and the oxidation of biogenic volatile organic compounds remain under-explored. Other specific comments or suggestions are as follows.

Response:

Although the initial concentrations of alkaline species used in the experiments were higher than the ambient levels, this consideration was necessary to tackle their influence on the mechanisms of chloride depletion within a short time scale. Many chamber experiments have indeed shown that the relatively high initial reactant concentration is important to clarify complex reaction processes in a short time scale

(Kong et al., 2024; Zhang et al., 2024). Due to the inherent limitations of laboratory chamber studies (e.g., wall effects), experiments of this nature are typically conducted over relatively short timescales. Consequently, the results obtained may be less pronounced than those observed in field measurements. In our specific experiments, the chloride depletion, measured after two hours of reaction, was lower than that observed in field measurements after extended atmospheric aging. For example, chloride depletion in the experiment without alkaline species (Exp. N.1) was 24.4%, lower than that observed in field studies (43-98%) (Cvitešić Kušan et al., 2020; Rastogi et al., 2020; Yu et al., 2021). After adding alkaline species, the weakening effect on chloride depletion was significant. In the actual atmospheric environment, longer reaction times would likely result in a more pronounced weakening effect of alkaline species on chloride depletion. Our findings suggest that alkaline species, more specifically organic amines, are significant factors influencing chloride depletion in the coastal atmosphere. This further supports the hypothesis from field studies that ammonia can reduce chloride depletion (Rankin and Wolff, 2003; Braun et al., 2017; Zhan et al., 2017; Chen et al., 2016; Yao et al., 2003; Ghosh et al., 2020).

Additionally, we would like to thank the Referee for raising this important question regarding quantifying the competitive kinetics between organic amine-acid neutralization and the oxidation of biogenic volatile organic compounds. The purpose of this study to identify organic chlorinated compounds is to provide evidence of their formation from chloride depletion in field observations. Notably, acid-base neutralization reactions indirectly affect the generation of organic chlorinated compounds by influencing the formation of active chlorine. Nevertheless, we used Framework for 0-D Atmospheric Modeling (F0AM) to further investigate the competition between HNO_3 and NH_3, as well as between HNO_3 and Cl^-. The acid-base neutralization reactions were incorporated into the mechanism. For example, the time series of the HNO_3 and Cl exposure were simulated using F0AM for Exp.N.1-NA.3 (Fig. S1). The exposure of HNO_3 and Cl decreased after the addition of NH_3, further supporting the crucial role of the reaction between NH_3 and HNO_3 in reducing chloride depletion. As the main oxidizing agent in the formation of organic chlorinated

compounds, the decrease in chlorine atoms concentration can further lead to the decline in the formation of organic chlorinated compounds. Since the rate of chlorine atoms (generated by chloride ion activation) transition into organochlorine products is not well understood and represents a significant research gap in atmospheric heterogeneous chemistry, this process is not included in the model. Our mass spectrometry results also confirmed that the formation of organic chlorinated compounds was reduced with NH_3 addition. Notably, the kinetic data of the most DMA and SO_2 related reactions are currently unavailable and, consequently, deserves the attention of future research. These have been clarified in the revised manuscript and Supplement.

Lines 80-82, Page 4:

Although the initial concentrations of alkaline species used in the experiments were higher than the ambient levels, this consideration was necessary for laboratory experiments within a short time scale to tackle their influence on chloride depletion.

Lines 154-161, Page 7-8:

2.3 Box model

The Framework for 0-D Atmospheric Modeling (F0AM) (Wolfe et al., 2016) was used to further investigate the impact of alkaline species on chloride depletion. The gas phase reactions used in this study were derived from the Master Chemical Mechanism (MCM) v3.3.1 (http://mcm.york.ac.uk/) (Jenkin et al., 2015). Based on the heterogeneous reactions integrated in our previous work (Song et al., 2026), we further incorporated the acid-base neutralization reactions into the mechanism, with a rate constant of 2.64×10^{-16} cm^3 $molecule^{-1}$ s^{-1} for the reaction between NH_3 and HNO_3 (Behera and Sharma, 2012). The initial conditions in the model were set to match those of the chamber experiments.

Lines 177-180, Page 8:

Furthermore, the time series of the HNO_3 and Cl atoms exposure were simulated using F0AM for Exp.N.1-NA.3 (Fig. S1). The exposure of HNO_3 and Cl atoms decreased after NH_3 addition, further supporting the crucial role of the reaction between NH_3 and HNO_3 in reducing chloride depletion.

Figure S1 in the Supplement:

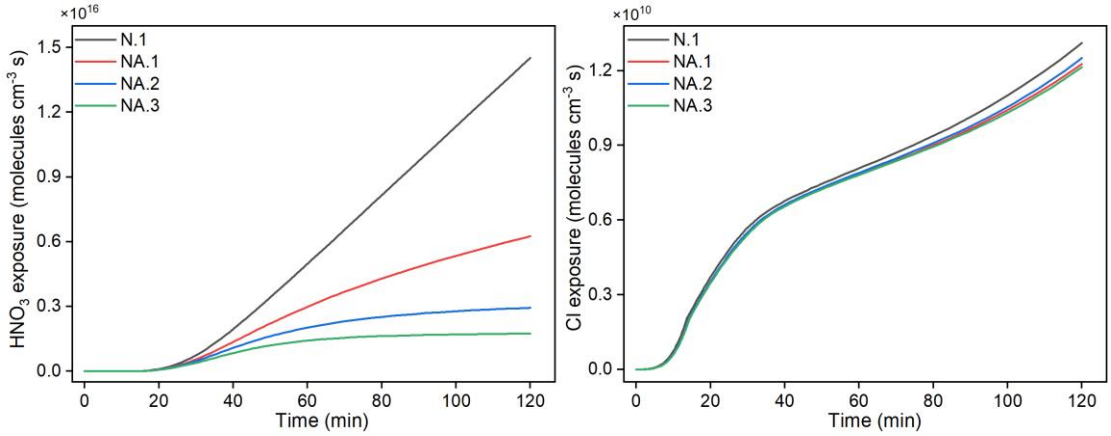

Figure S1. Time series of HNO_3 and Cl exposure for Exp.N.1-NA.3 obtained from model simulation.

2. It would be better to explicitly cite recent studies and specific uncertainties highlighting the gap to predict Cl-depletion in amine-rich coastal or agricultural-marine interfaces. This frames the paper as a "missing piece" of the global chlorine budget.

Response:

Data from modeled and observed chloride depletion were extracted from previous studies (Nolte et al., 2015; Su et al., 2022). According to the calculation analysis, the average value of the absolute difference between chloride depletion from field observations and from model predictions is determined to be 20%, while the maximum value can be as high as 97%. Notably, the influence of organic amines has not been taken into account in the model's prediction of chloride, highlighting the gap to predict chloride depletion in amine-rich coastal or agricultural-marine interfaces. This has been updated in the revised manuscript.

Lines 38-41, Page 2-3:

However, significant discrepancies exist between field observations and model predictions of chloride depletion with an average absolute difference of 20% (Nolte et al., 2008; Nolte et al., 2015; Su et al., 2022), highlighting the need for a deeper understanding of its underlying mechanisms.

Lines 52-54, Page 3:

The influence of organic amines remains overlooked in model predictions (Nolte et al., 2015), highlighting a critical gap for accurately predicting chloride depletion in amine-rich coastal or agricultural-marine interfaces.

3. Discuss the shifting ratio of ammonia to organic amines in diverse coastal environments to emphasize the global relevance of the findings beyond a single simulated environment.

Response:

It is reported that NH_3 concentrations range from <0.6 to 123 nmol m^{-3} with maxima around local noon and minima near dawn in coastal New England during summer (Smith et al., 2007). Chen et al. (2022) found an average (± standard deviation) NH_3 concentration of 1.2 ± 1.3 μg m^{-3} along the coastline of eastern China, while an average atmospheric NH_3 concentration of 1.24 ± 0.98 μg m^{-3} was determined in a coastal urban airshed (Berner and David Felix, 2020). The average concentration range of total organic amines in different coastal areas is 19-130 ng m^{-3} (Liu et al., 2022; Liu et al., 2024; Liu et al., 2023; Du et al., 2021). This leads to a shifting ratio range of 0.1-110 for ammonia to organic amines in diverse coastal environments. In this study, the shifting ratio range of ammonia to organic amines used was 0.67-6, which falls within the ranges observed in diverse coastal environments. This indicates the global relevance of our findings. We clarified this in the revised manuscript.

Lines 77-80, Page 4:

Here, the shifting ratios of ammonia to DMA are in the range 0.67-6, which falls within the ranges observed in diverse coastal environments (0.1-110) (Smith et al., 2007; Chen et al., 2022; Berner and David Felix, 2020; Liu et al., 2022; Liu et al., 2024; Liu et al., 2023; Du et al., 2021).

4. Perform a "bridge" experiment or use kinetic modeling to demonstrate that the observed mechanisms persist at near-ambient (1 – 5 ppb) concentrations, thereby validating the atmospheric scalability of the results. Additionally, it would be beneficial

to review the current field observations of chlorine depletion data to determine whether the chlorine depletion measured in laboratories can, to some extent, explain the observed values under actual atmospheric conditions.

Response:

To quickly tackle the mechanism by which alkaline species affect chloride depletion, we used initial concentrations of alkaline species that were higher than the ambient levels. In most chamber experiments, the relatively high initial reactant concentration is important to clarify complex reaction processes in a short time scale (Kong et al., 2024; Zhang et al., 2024). The current laboratory approach often relies on using high reactant concentrations to accelerate reaction kinetics over short timescales (Kong et al., 2024; Zhang et al., 2024), thereby generating detectable signals to infer mechanisms that occur over longer periods at low concentrations in the ambient air. Reducing the reactant concentrations to near-ambient levels (1–5 ppb) would result in extremely low extents of heterogeneous reactions within our experimental timeframe. The product yields would likely fall below the detection limits of our current analytical instruments, precluding the acquisition of reliable kinetic or mechanistic data. This represents a common technical bottleneck in laboratory studies. Nevertheless, we used Framework for 0-D Atmospheric Modeling (F0AM) to further investigate the impact of alkaline species on chloride depletion at near-ambient concentrations. As shown in Table S1, the exposure of HNO_3 and Cl atoms also decreased after NH_3 addition (0-20 ppb), demonstrating that the crucial role of the reaction between NH_3 and HNO_3 in reducing chloride depletion persists at near-ambient concentrations.

Many field observation studies have hypothesized that ammonia can reduce chloride depletion (Rankin and Wolff, 2003; Yao et al., 2003; Braun et al., 2017; Ghosh et al., 2020). For example, a relatively low level of chloride depletion (8%) was observed in the Antarctic winter, and the high levels of ammonia emitted by penguins has been hypothesized to be responsible for this phenomenon (Rankin and Wolff, 2003). Braun et al. (2017) postulated that the lower levels of particulate NH_4^+ during FASE allowed for greater Cl^- depletion by SO_4^{2-}. Zhan et al. (2017) found that in some

samples showing a reduction in chloride depletion, the concentrations of ammonium ions (mainly resulting from ammonia emissions) were relatively low., A relatively weak chloride depletion was observed in Guangzhou in southern China, with values of 72 % and 47 % in fine and coarse mode particle, respectively, despite the relatively high concentration of ammonium ions (Chen et al., 2016). However, no relationship between chloride depletion and organic amines has yet been established from existing field observation studies.

The current study conducted laboratory experiments to investigate the extent of the influence of two types of important alkaline species (NH_3 and DMA) on chloride depletion, and analyzed the underlying mechanisms of their effects. Results showed that alkaline species could weaken chloride depletion caused by acidic gases, mainly due to acid-base neutralization. Our findings suggest that alkaline species, more specifically organic amines, significantly influence chloride depletion in the coastal atmosphere. This further supports the hypothesis from the field studies that ammonia can reduce chloride depletion. Updates have been made in the revised manuscript and Supplement.

Lines 177-182, Page 8:

Furthermore, the time series of the HNO_3 and Cl atoms exposure were simulated using F0AM for Exp.N.1-NA.3 (Fig. S1). The exposure of HNO_3 and Cl atoms decreased after NH_3 addition, further supporting the crucial role of the reaction between NH_3 and HNO_3 in reducing chloride depletion. As shown in Table S1, the exposure of HNO_3 and Cl atoms also decreased after the addition of NH_3 (0-20 ppb), demonstrating that the observed mechanisms persist at near-ambient concentrations.

Lines 191-194, Page 9:

Our findings further support the hypothesis formulated from field studies that ammonia can reduce chloride depletion (Rankin and Wolff, 2003; Braun et al., 2017; Zhan et al., 2017; Chen et al., 2016; Yao et al., 2003; Ghosh et al., 2020).

Table S1 in the Supplement:

Table S1. Summary of model simulation conditions and results.

Experiment[a]	$[NO_x]_0$ (ppb)	$[NH_3]_0$ (ppb)	HNO_3 exposure (molecules cm^{-3} s)	Cl exposure (molecules cm^{-3} s)
NA.0	50	0	3.35439e+015	1.05106e+010
NA.5	50	5	3.12956e+015	1.0508e+010
NA.20	50	20	2.5492e+015	1.05006e+010

[a]Abbreviations used in experimental codes correspond to the reactants introduced into the model. "N" represents NO_x, and "A" represents NH_3. "NA.0-NA.20" represent 0 ppb – 20 ppb NH_3 concentrations, with a fixed initial NO_x concentration of 50 ppb.

5. Since SSAs transition between aqueous and semi-solid states, how does this affect the neutralization efficiency of DMA compared to the more mobile ammonia should be discussed.

Response:

The neutralization efficiency of alkaline species can be affected by the particle phase state. When the phase state of particles changes from liquid to semisolid state, the neutralization efficiency of DMA may be relatively inhibited compared to the more mobile NH_3 (Sauerwein and Chan, 2017; Derieux et al., 2019). This can be attributed to the fact that ammonia is a relatively light and highly mobile molecule, being capable of diffusing into semisolid particles more effectively than DMA. To verify the phase changes of SSA in this study and evaluate their effects on NH_3 and DMA neutralization, we calculated the viscosity of the particles. Using the approach by Tumminello et al., (Tumminello et al., 2021), we determined the viscosity of SSA particles in our experiments to be 1.89-1.98 Pa·s (details in the Supplement), which is significantly lower than the 10^2 Pa·s threshold for liquid-to-semisolid phase transition (Derieux et al., 2018). This suggests that the SSA particles existed in liquid state in our experiments, and the neutralization efficiency of both ammonia and DMA was not constrained by phase transition. Clarifications have been made in the revised manuscript and Supplement.

Lines 233-241, Page 10-11:

Notably, the neutralization efficiency of alkaline species can be affected by the particle phase state. When the phase state of particles changes from liquid to semisolid state, the neutralization efficiency of DMA may be relatively inhibited compared to that of the more mobile NH_3 (Sauerwein and Chan, 2017; Derieux et al., 2019). The viscosity of SSA particles in our experiments was calculated to be 1.89-1.98 Pa·s (details in the Supplement), being significantly lower than the 10^2 Pa·s threshold for liquid-to-semisolid phase transition (Derieux et al., 2018). This suggests that the SSA particles in this study existed in liquid state, and the neutralization efficiency of both ammonia and DMA was not constrained by phase transition.

Section S1 in the Supplement:

S1. Calculation of particle viscosity

The dry glass transition temperature of the organic components ($T_{g,org}$) in SSA particles was first calculated using the number of carbon, hydrogen, and oxygen atoms (n_C, n_H, and n_O):

$$T_{g,org}=\left(n_C^0+ln(n_C)\right)b_C+ln(n_H)b_H+ln(n_C)ln(n_H)b_{CH}+ln(n_O)b_O+ln(n_C)ln(n_O)b_{CO} \quad \text{(S1)}$$

Here, the values of n_C^0, b_C, b_H and b_O,b_{CH} and b_{CO} are best-fit parameters presented in Derieux et al. (2018). Then, the average glass transition temperature of organic–water mixtures ($T_{g,org,w}$) can be calculated using the Gordon-Taylor equation (Derieux et al., 2018; Tumminello et al., 2021):

$$T_{g,org,w}=\frac{T_{g,w}f_{ALW}+\frac{1}{k_{GT}}f_{org}T_{g,org}}{f_{ALW}+\frac{1}{k_{GT}}f_{org}} \quad \text{(S2)}$$

$$f_{ALW}=\frac{m_{w,org}}{m_{w,org}+m_{org}} \quad \text{(S3)}$$

where $T_{g,w}$ and k_{GT} are the glass transition temperature of water (136 K) and the Gordon-Taylor constant (1), respectively. $m_{w,org}$ and m_{org} refer to the mass of water and organic components, respectively. Subsequently, the viscosity of the organic component (η_{org}) can be obtained through the conversion of $T_{g,org,w}$ using Eq.S4 and Eq.S5. Among them, the fragility parameter (z) was assumed to be 12 (Tumminello et al., 2021). T is the experimental temperature.

$$T_0=\frac{39.17T_{g,org,w}}{z+39.17} \quad \text{(S4)}$$

$$log\eta_{org}=-5+0.434\frac{T_0 z}{T-T_0} \quad (S5)$$

For the viscosity of inorganic components (η_{iorg}), calculations can be performed using the viscosity of water at 25°C (η_w, 0.8904 cP), the mole fraction of cations in the solution (X_c), the free energy associated with NaCl (E), and the molar volume of the hole formed by the movement of cations and anions (V):

$$\eta_{inorg}=\frac{\eta_w e^{X_c E}}{1+X_c V} \quad (S6)$$

where E and V are determined from the data presented by Goldsack and Franchetto (1977).

Finally, the SSA particle viscosity (η_{mix}) calculated by Eq.S7 based on the assumption that the organic and inorganic components of SSA particles are homogeneous and internally-mixed (Tumminello et al., 2021).

$$ln(\eta_{mix})=\sum_{i=1}^{N} x_i ln(\eta_i) \quad (S7)$$

Here, x_i and η_i are the mole fraction and viscosity of component i (organic or inorganic components), respectively.

Additionally, the Extended AIM Aerosol Thermodynamics Model (E-AIM, https://www.aim.env.uea.ac.uk/aim/aim.php) was used to assess the content of the components of SSA particles.

6. Quantify the branching ratio between the formation of organochlorines and the simple neutralization of salts. Additionally, whether the products simulated in these experiments can correspond to the organochlorine species observed in field observations may also serve as one piece of evidence bridging laboratory and field studies.

Response:

As stated in answer to the first question, the acid-base neutralization reactions indirectly affect the generation of organic chlorinated compounds by influencing the formation of active chlorine. The purpose of this study to identify organic chlorinated compounds is to provide evidence of their formation from chloride depletion in field observations. Nevertheless, we used Framework for 0-D Atmospheric Modeling

(F0AM) to further investigate the competition between HNO_3 and NH_3, as well as between HNO_3 and Cl^-. The acid-base neutralization reactions were incorporated into the mechanism. For example, the time series of the HNO_3 and Cl exposure were simulated using F0AM for Exp.N.1-NA.3 (Fig. S1). The exposure of HNO_3 and Cl atoms decreased after the addition of NH_3, further supporting the crucial role of the reaction between NH_3 and HNO_3 in reducing chloride depletion. As the main oxidizing agent in the formation of organic chlorinated compounds, the decrease in Cl atoms concentration can further lead to the decline in the formation of organic chlorinated compounds. Since the rate of chlorine atoms (generated by chloride ion activation) transition into organochlorine products is not well understood and represents a significant research gap in atmospheric heterogeneous chemistry, this process is not included in the model. Our mass spectrometry results also confirmed that the formation of organic chlorinated compounds was reduced with NH_3 addition.

Additionally, we detected products (e.g., $C_5H_7ClO_4$, $C_8H_{11}ClO_5$, and $C_8H_{13}ClO_6$) that could correspond to organochlorine species observed in field observations, indicating that reactive chlorine produced from chloride depletion serves as a critical oxidant for the formation of organic chlorinated compounds (Chen et al., 2023). These products were identified in our previous study (Song et al., 2026), and their formation pathways were proposed.

This has been updated in the revised manuscript and Supplement.

Lines 154-161, Page 7-8:

2.3 Box model

The Framework for 0-D Atmospheric Modeling (F0AM) (Wolfe et al., 2016) was used to further investigate the impact of alkaline species on chloride depletion. The gas phase reactions used in this study were derived from the Master Chemical Mechanism (MCM) v3.3.1 (http://mcm.york.ac.uk/) (Jenkin et al., 2015). Based on the heterogeneous reactions integrated in our previous work (Song et al., 2026), we further incorporated the acid-base neutralization reactions into the mechanism, with a rate constant of 2.64×10^{-16} cm^3 $molecule^{-1}$ s^{-1} for the reaction between NH_3 and HNO_3 (Behera and Sharma, 2012). The initial conditions in the model were set to match those

of the chamber experiments.

Lines 177-180, Page 8:

Furthermore, the time series of the HNO_3 and Cl atoms exposure were simulated using F0AM for Exp.N.1-NA.3 (Fig. S1). The exposure of HNO_3 and Cl atoms decreased after NH_3 addition, further supporting the crucial role of the reaction between NH_3 and HNO_3 in reducing chloride depletion.

Lines 286-290, Page 12-13:

Some organic chlorinated compounds (e.g., $C_5H_7ClO_4$, $C_8H_{11}ClO_5$, and $C_8H_{13}ClO_6$) detected in this study have also been reported in field observations (Chen et al., 2023), indicating that chloride depletion could be a source thereof in the ambient environment. These compounds were identified in our previous study and their formation pathways were proposed (Song et al., 2026).

Figure S1 in the Supplement:

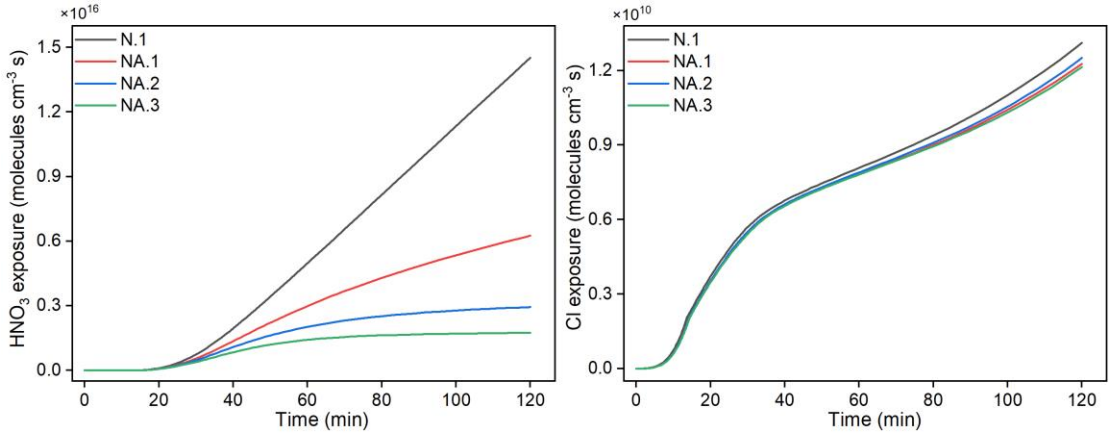

Figure S1. Time series of HNO_3 and Cl exposure for Exp.N.1-NA.3 obtained from model simulation.

7. I suggest to briefly discuss the toxicological implications of the identified organochlorine compounds, as their stabilization in the particle phase (due to higher pH) might increase their persistence and long-range transport potential.

Response:

We have discussed toxicity for of identified organic chlorinated compounds based on their possible chemical structures. Using Toxicity Estimation Software Tool

(T.E.S.T., V.5.1.2, USEPA), their oral rat pLD_{50} ($-\log_{10}$(pred), mol kg^{-1}), developmental toxicity, and mutagenicity were estimated. Table S2 presents detailed toxicity prediction results for possible chemical structures of identified organic chlorinated compounds. Results show that $C_7H_{13}ClN_2O_4$ have the highest pLD_{50} values and are classified as class 3, indicating that they have considerable potential for acute toxicity. Notably, the predicted developmental toxicity values for the compounds listed in Table S2 have been classified as the highest hazard level, and they also pose risks of mutagenicity. This indicates the necessity to conduct in-depth research on the toxicity of organic chlorinated compounds in the coastal atmosphere. These toxicological implications have been clarified in the revised manuscript and Supplement.

Lines 151-153, Page 7 in the revised manuscript:

The toxicity of identified organic chlorinated compounds was analyzed based on their possible chemical structures using Toxicity Estimation Software Tool (T.E.S.T., V.5.1.2, USEPA) to estimate their oral rat pLD_{50} ($-\log_{10}$(pred), mol kg^{-1}), developmental toxicity, and mutagenicity.

Lines 320-325, Page 14 in the revised manuscript:

The toxicity prediction results of these organic chlorinated compounds are presented in Table S2. Results show that $C_7H_{13}ClN_2O_4$ compounds have the highest pLD_{50} values and are classified as class 3, indicating that they have considerable potential for acute toxicity. Notably, the predicted developmental toxicity values for the compounds listed in Table S2 have been classified as the highest hazard level, and they also pose mutagenicity risks. This highlights the necessity to conduct in-depth research on the toxicity of organic chlorinated compounds in the coastal atmosphere.

Table S2 in the Supplement:

Table S2. Toxicity prediction results for chemical structures of identified organic chlorinated compounds.

Molecular formula	Oral rat pLD_{50} (-log10(pred), mol kg^{-1})	pLD50 level*	Pred Developmental Toxicity**	Pred Mutagenicity**
$C_9H_{14}ClNO_9$	2.29	class 4	N/A	N/A

$C_7H_{13}ClN_2O_4$	2.61	class 3	0.80	0.33
$C_7H_{13}ClN_2O_9$	2.29	class 4	0.83	0.49
$C_6H_{10}ClNO_3$	1.74	class 4	0.77	0.24
$C_6H_{10}ClNO_4$	2.36	class 4	0.78	0.99
$C_7H_{14}ClNO_3$	2.29	class 4	0.80	0.95
$C_7H_{13}Cl_2NO_3$	1.56	class 5	0.66	0.07

*The class levels can be divided into five categories: class 1 (highest hazard, $pLD_{50} \geq 4.3$), class 2 ($4.3 > pLD_{50} > 3.3$), class 3 ($3.3 > pLD_{50} > 2.5$), class 4 ($2.5 > pLD_{50} > 1.69$), and class 5 (likely hazard, $1.69 > pLD_{50} > 1.3$) (Europe, 2021; Li et al., 2025).

**The class levels can be divided into two categories: class 1 (highest hazard, > 0.5), and class 2 (likely hazard, ≤0.5) (Europe, 2021; Li et al., 2025).

References

Behera, S. N. and Sharma, M.: Transformation of atmospheric ammonia and acid gases into components of $PM_{2.5}$: An environmental chamber study, Environ Sci Pollut Res 19, 1187-1197, https://doi.org/10.1007/s11356-011-0635-9, 2012.

Berner, A. H. and David Felix, J.: Investigating ammonia emissions in a coastal urban airshed using stable isotope techniques, Sci. Total Environ., 707, 134952, https://doi.org/10.1016/j.scitotenv.2019.134952, 2020.

Braun, R. A., Dadashazar, H., MacDonald, A. B., Aldhaif, A. M., Maudlin, L. C., Crosbie, E., Aghdam, M. A., Hossein Mardi, A., and Sorooshian, A.: Impact of wildfire emissions on chloride and bromide depletion in marine aerosol particles, Environ. Sci. Technol., 51, 9013-9021, https://doi.org/10.1021/acs.est.7b02039, 2017.

Chen, D., Yao, X., Chan, C. K., Tian, X., Chu, Y., Clegg, S. L., Shen, Y., Gao, Y., and Gao, H.: Competitive uptake of dimethylamine and trimethylamine against ammonia on acidic particles in marine atmospheres, Environ. Sci. Technol., 56, 5430-5439, https://doi.org/10.1021/acs.est.1c08713, 2022.

Chen, H., Yan, C., Fu, Q., Wang, X., Tang, J., Jiang, B., Sun, H., Luan, T., Yang, Q., Zhao, Q., Li, J., Zhang, G., Zheng, M., Zhou, X., Chen, B., Du, L., Zhou, R., Zhou, T., and Xue, L.: Optical properties and molecular composition of wintertime atmospheric water-soluble organic carbon in different coastal cities of eastern China, Sci. Total Environ., 892, 164702, https://doi.org/10.1016/j.scitotenv.2023.164702, 2023.

Chen, W., Wang, X., Cohen, J. B., Zhou, S., Zhang, Z., Chang, M., and Chan, C.-Y.: Properties of aerosols and formation mechanisms over southern China during the monsoon season, Atmos. Chem. Phys., 16, 13271-13289, https://doi.org/10.5194/acp-16-13271-2016, 2016.

Cvitešić Kušan, A., Kroflič, A., Grgić, I., Ciglenečki, I., and Frka, S.: Chemical characterization of fine aerosols in respect to water-soluble ions at the eastern Middle Adriatic coast, Environ Sci Pollut R., 27, 10249-10264, https://doi.org/10.1007/s11356-020-07617-7, 2020.

DeRieux, W.-S. W., Lakey, P. S. J., Chu, Y., Chan, C. K., Glicker, H. S., Smith, J. N., Zuend, A., and Shiraiwa, M.: Effects of phase state and phase separation on

dimethylamine uptake of ammonium sulfate and ammonium sulfate–sucrose mixed particles, ACS Earth Space Chem., 3, 1268-1278, https://doi.org/10.1021/acsearthspacechem.9b00142, 2019.

DeRieux, W.-S. W., Li, Y., Lin, P., Laskin, J., Laskin, A., Bertram, A. K., Nizkorodov, S. A., and Shiraiwa, M.: Predicting the glass transition temperature and viscosity of secondary organic material using molecular composition, Atmos. Chem. Phys., 18, 6331-6351, https://doi.org/10.5194/acp-18-6331-2018, 2018.

Du, W., Wang, X., Yang, F., Bai, K., Wu, C., Liu, S., Wang, F., Lv, S., Chen, Y., Wang, J., Liu, W., Wang, L., Chen, X., and Wang, G.: Particulate amines in the background atmosphere of the Yangtze River Delta, China: Concentration, size distribution, and sources, Adv. Atmos. Sci., 38, 1128-1140, https://doi.org/10.1007/s00376-021-0274-0, 2021.

Europe, U. N. E. C. f.: Globally Harmonized System of Classification and Labelling of Chemicals (GHS), Glob. Harmon. Syst. Classif. Label. Chem. (GHS), https://doi.org/10.18356/9789210052139, 2021.

Ghosh, A., Roy, A., Das, S. K., Ghosh, S. K., Raha, S., and Chatterjee, A.: Identification of most preferable reaction pathways for chloride depletion from size segregated sea-salt aerosols: A study over high altitude Himalaya, tropical urban metropolis and tropical coastal mangrove forest in eastern India, Chemosphere, 245, 125673, https://doi.org/10.1016/j.chemosphere.2019.125673, 2020.

Goldsack, D. E. and Franchetto, R.: The viscosity of concentrated electrolyte solutions. I. Concentration dependence at fixed temperature, Can J. Chem., 55, 1062-1070, https://doi.org/10.1139/v77-148, 1977.

Jenkin, M. E., Young, J. C., and Rickard, A. R.: The MCM v3.3.1 degradation scheme for isoprene, Atmos. Chem. Phys., 15, 11433-11459, https://doi.org/10.5194/acp-15-11433-2015, 2015.

Kong, X., Wu, C., Mishra, H. R., Hao, Y., Cazaunau, M., Bergé, A., Pangui, E., Faust, R., Liu, W., Li, J., Wang, S., Picquet-Varrault, B., and Hallquist, M.: Impact of SO_2 and light on chemical morphology and hygroscopicity of natural salt aerosols, Atmospheric Environment, 322, 120373, https://doi.org/10.1016/j.atmosenv.2024.120373, 2024.

Li, C., Yao, L., Wang, Y., Fang, M., Chen, X., Wang, L., Li, Y., Yang, G., and Wang, L.: Formation of chlorinated organic compounds from Cl atom-initiated reactions of aromatics and their detection in suburban Shanghai, Atmos. Chem. Phys., 25, 11247-11260, https://doi.org/10.5194/acp-25-11247-2025, 2025.

Liu, M., Wang, X., Liu, Z., Jiang, Y., Li, M., Zhang, J., Sun, Y., Zhu, Y., Xue, L., and Wang, W.: Characteristics and origins of fine particulate amines at a coastal mountain site in northern China in spring, Atmos. Environ., 321, 120365, https://doi.org/10.1016/j.atmosenv.2024.120365, 2024.

Liu, T., Xu, Y., Sun, Q. B., Xiao, H. W., Zhu, R. G., Li, C. X., Li, Z. Y., Zhang, K. Q., Sun, C. X., and Xiao, H. Y.: Characteristics, origins, and atmospheric processes of amines in fine aerosol particles in winter in China, J. Geophys. Res. Atmos., 128, e2023JD038974, https://doi.org/10.1029/2023jd038974, 2023.

Liu, Z., Li, M., Wang, X., Liang, Y., Jiang, Y., Chen, J., Mu, J., Zhu, Y., Meng, H., Yang, L., Hou, K., Wang, Y., and Xue, L.: Large contributions of anthropogenic sources to amines in fine particles at a coastal area in northern China in winter, Sci. Total Environ., 839, 156281, https://doi.org/10.1016/j.scitotenv.2022.156281, 2022.

Nolte, C., Bhave, P., Arnold, J., Dennis, R., Zhang, K., and Wexler, A.: Modeling urban and regional aerosols—Application of the CMAQ-UCD aerosol model to Tampa, a coastal urban site, Atmos. Environ., 42, 3179-3191, https://doi.org/10.1016/j.atmosenv.2007.12.059, 2008.

Nolte, C. G., Appel, K. W., Kelly, J. T., Bhave, P. V., Fahey, K. M., Collett Jr., J. L., Zhang, L., and Young, J. O.: Evaluation of the Community Multiscale Air Quality (CMAQ) model v5.0 against size-resolved measurements of inorganic particle composition across sites in North America, Geosci. Model Dev., 8, 2877-2892, https://doi.org/10.5194/gmd-8-2877-2015, 2015.

Rankin, A. M. and Wolff, E. W.: A year-long record of size-segregated aerosol composition at Halley, Antarctica, J. Geophys. Res. Atmos., 108, 4775, https://doi.org/10.1029/2003jd003993, 2003.

Rastogi, N., Agnihotri, R., Sawlani, R., Patel, A., Babu, S. S., and Satish, R.: Chemical and isotopic characteristics of PM_{10} over the Bay of Bengal: Effects of continental

outflow on a marine environment, Sci Total Environ., 726, 138438, https://doi.org/10.1016/j.scitotenv.2020.138438, 2020.

Sauerwein, M. and Chan, C. K.: Heterogeneous uptake of ammonia and dimethylamine into sulfuric and oxalic acid particles, Atmos. Chem. Phys., 17, 6323-6339, https://doi.org/10.5194/acp-17-6323-2017, 2017.

Smith, A. M., Keene, W. C., Maben, J. R., Pszenny, A. A. P., Fischer, E., and Stohl, A.: Ammonia sources, transport, transformation, and deposition in coastal New England during summer, J. Geophys. Res. Atmos., 112, https://doi.org/10.1029/2006jd007574, 2007.

Song, A., Li, K., Yang, Z., Xu, L., Chen, X., Tsona Tchinda, N., and Du, L.: Anthropogenic-Biogenic interaction drives chloride depletion in coastal atmospheres, under review, 2026.

Su, B., Wang, T., Zhang, G., Liang, Y., Lv, C., Hu, Y., Li, L., Zhou, Z., Wang, X., and Bi, X.: A review of atmospheric aging of sea spray aerosols: Potential factors affecting chloride depletion, Atmos. Environ., 290, 119365, https://doi.org/10.1016/j.atmosenv.2022.119365, 2022.

Tumminello, P. R., James, R. C., Kruse, S., Kawasaki, A., Cooper, A., Guadalupe-Diaz, I., Zepeda, K. L., Crocker, D. R., Mayer, K. J., Sauer, J. S., Lee, C., Prather, K. A., and Slade, J. H.: Evolution of sea spray aerosol particle phase state across a phytoplankton bloom, ACS Earth Space Chem., 5, 2995-3007, https://doi.org/10.1021/acsearthspacechem.1c00186, 2021.

Wolfe, G. M., Marvin, M. R., Roberts, S. J., Travis, K. R., and Liao, J.: The Framework for 0-D Atmospheric Modeling (F0AM) v3.1, Geosci. Model Dev., 9, 3309-3319, https://doi.org/10.5194/gmd-9-3309-2016, 2016.

Yao, X., Fang, M., and Chan, C. K.: The size dependence of chloride depletion in fine and coarse sea-salt particles, Atmos. Environ., 37, 743-751, https://doi.org/10.1016/S1352-2310(02)00955-X, 2003.

Yu, C., Yan, J., Zhang, H., Lin, Q., Zheng, H., Zhao, S., Zhong, X., Zhao, S., Zhang, M., and Chen, L.: Chemical characteristics of sulfur-containing aerosol particles across the western North Pacific and the Arctic Ocean, Atmos. Res., 253, 105480,

https://doi.org/10.1016/j.atmosres.2021.105480, 2021.

Zhan, J., Li, W., Chen, L., Lin, Q., and Gao, Y.: Anthropogenic influences on aerosols at Ny-Ålesund in the summer Arctic, Atmos. Pollut. Res., 8, 383-393, https://doi.org/10.1016/j.apr.2016.10.010, 2017.

Zhang, Z., Zhao, Y., Zhao, Y., Zang, X., Xie, H., Yang, J., Zhang, W., Wu, G., Li, G., Yang, X., and Jiang, L.: Effects of NO and SO_2 on the secondary organic aerosol formation from isoprene photooxidation, Atmos. Environ., 318, 120248, https://doi.org/10.1016/j.atmosenv.2023.120248, 2024.